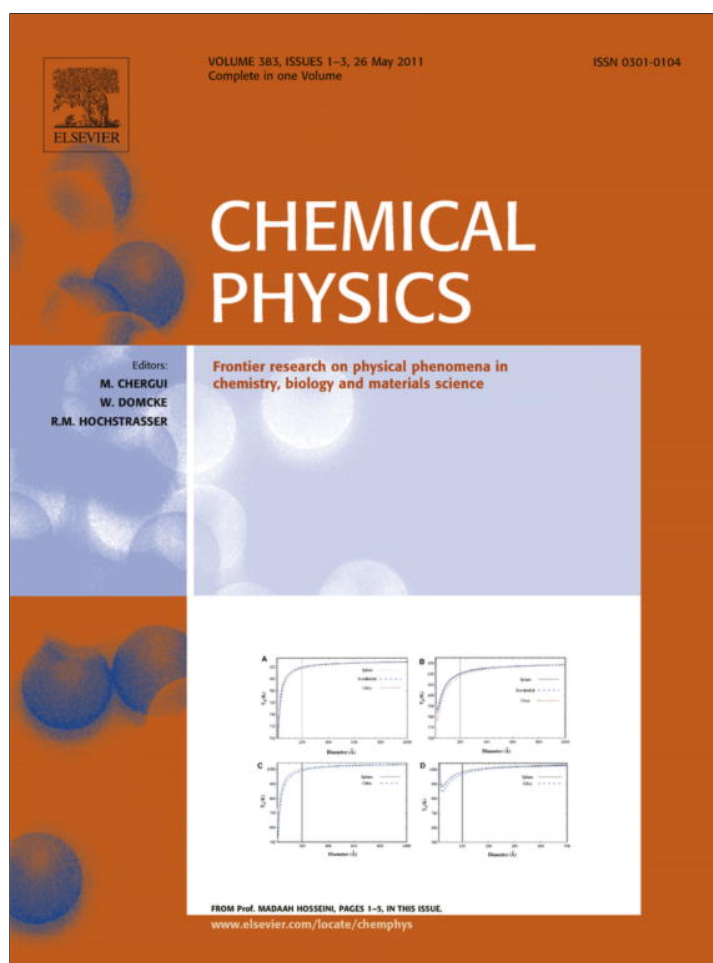


Provided for non-commercial research and education use.  
Not for reproduction, distribution or commercial use.



This article appeared in a journal published by Elsevier. The attached copy is furnished to the author for internal non-commercial research and education use, including for instruction at the authors institution and sharing with colleagues.

Other uses, including reproduction and distribution, or selling or licensing copies, or posting to personal, institutional or third party websites are prohibited.

In most cases authors are permitted to post their version of the article (e.g. in Word or Tex form) to their personal website or institutional repository. Authors requiring further information regarding Elsevier's archiving and manuscript policies are encouraged to visit:

<http://www.elsevier.com/copyright>



Contents lists available at ScienceDirect

## Chemical Physics

journal homepage: [www.elsevier.com/locate/chemphys](http://www.elsevier.com/locate/chemphys)

## Lateral interaction and structures in Cl adlayers on the Ag(111) surface

N.V. Petrova\*, I.N. Yakovkin, O.M. Braun

Institute of Physics, National Academy of Sciences of Ukraine, Prospect Nauki 46, Kiev 03028, Ukraine

## ARTICLE INFO

## Article history:

Received 9 January 2011  
In final form 28 March 2011  
Available online 3 April 2011

## Keywords:

DFT calculations  
Monte Carlo simulations  
Lateral interaction  
Adsorption  
Structure  
Silver  
Chlorine

## ABSTRACT

The lateral interaction and formation of ordered structures in Cl submonolayers adsorbed on Ag(111) surface at low coverages (up to 0.5 ML), when the diffusion of Cl into the bulk is negligible, have been studied by Monte Carlo method using parameters of the lateral interaction estimated from DFT calculations. The transition temperature and sharpness of the order–disorder transition for the  $(\sqrt{3} \times \sqrt{3})R30^\circ$  structure, derived from the Monte Carlo simulation, are in good agreement with available experimental data. It has been demonstrated that a restricted mobility of adsorbed Cl atoms can result, for a relatively high rate of the cooling of the layer, in the formation of domain structures. For imperfect domain structures, the model LEED patterns show a characteristic splitting of reflections due to phase shifts for electrons scattered at different domains.

© 2011 Elsevier B.V. All rights reserved.

## 1. Introduction

Chlorine serves as a promoter of the selective epoxidation of ethylene on Ag surfaces, widely used as catalysts in the chemical industry. The importance of a detailed knowledge of mechanisms of the reaction has stimulated extensive studies of the structural and kinetic properties of chlorine layers adsorbed on various Ag surfaces [1–21]. In particular, the adsorption of chlorine on the Ag(111) surface has been studied both theoretically and experimentally by different techniques including low energy electron diffraction (LEED) [1–5], surface extended X-ray absorption fine structure (SEXAFS) [5,14], Auger spectroscopy [1–3], thermal desorption [2,3], scanning tunneling microscopy [4,13,15], temperature programmed X-ray photoelectron spectroscopy (TPXPS) [16], and by DFT calculations [17–22].

It is well established that the adsorption of chlorine on Ag(111) proceeds with the dissociation of  $\text{Cl}_2$  molecules (an exothermic reaction with an almost vanishing barrier of 0.03 eV [21]). The initial sticking probability of Cl on the Ag(111) is of 0.4 [3], and at room temperature for coverages  $\theta$  up to 0.5 monolayer (ML), chlorine does not diffuse into the substrate, so that adsorbed Cl atoms remain on the surface [16,21,22]. At low coverages, the bonding of the Cl with the Ag(111) surface is rather strong (2.9–3.0 eV for  $\theta = 0.33$  ML in the  $(\sqrt{3} \times \sqrt{3})R30^\circ$  structure [17]) and exceeds the energy of dissociation of the  $\text{Cl}_2$  molecule (2.476 eV [21]). This relation of binding energies, according to the rule suggested for dia-

atomic gases [2,23], ultimately indicates that for low coverages (about 0.33 ML) Cl will desorb in an atomic form (i.e., without a recombination in  $\text{Cl}_2$  molecules).

For higher Cl coverages ( $\theta > 0.5$ ) and temperatures of 300–600 K, the Ag(111) surface reconstructs forming an array of triangle-shaped islands having the  $(3 \times 3)$  symmetry [13], surrounded by the  $(\sqrt{3} \times \sqrt{3})R30^\circ$  structure. With increasing coverage, the formation of  $\text{Cl}_3\text{Ag}$  clusters was observed at the boundaries of the domains of the  $(3 \times 3)$  structure. The maximal Cl coverage on Ag(111) was found to be of 0.55, and chlorine desorbs from the surface (at 650–780 K) as silver chloride clusters [3,16].

The low energy electron diffraction (LEED) study of Cl on Ag(111) [1–5], performed at room temperature, did not reveal the formation of ordered structures at low coverages. A well-defined LEED pattern appears only for the coverage slightly below saturation. It should be noted that there is no consensus in the literature about the periodicity of this structure, and the coverage that corresponds to the saturation of adsorption is still under debates [14,15]. At lower temperatures, however, Cl on Ag(111) forms the  $(\sqrt{3} \times \sqrt{3})R30^\circ$  structure at  $\theta = 0.33$  [5] (Fig. 1 a) and, as follows from DFT calculations [19,21], could form a hexagonal honeycomb structure at  $\theta = 0.5$  (Fig. 1 b).

Shard and Dhanak [5] have performed a LEED study of the formation of the  $(\sqrt{3} \times \sqrt{3})R30^\circ$  Cl structure on the Ag(111) surface as a function of temperature. At low temperatures, a sharp LEED pattern indicated the formation of a well-ordered structure, while for temperatures above 195 K the fractional order spots abruptly became diffuse thus indicating a disordered structure. The order–disorder transition was found to be quite sharp (the temperature range of the transition is  $\sim 2$  K).

\* Corresponding author.

E-mail address: [petrova@iop.kiev.ua](mailto:petrova@iop.kiev.ua) (N.V. Petrova).

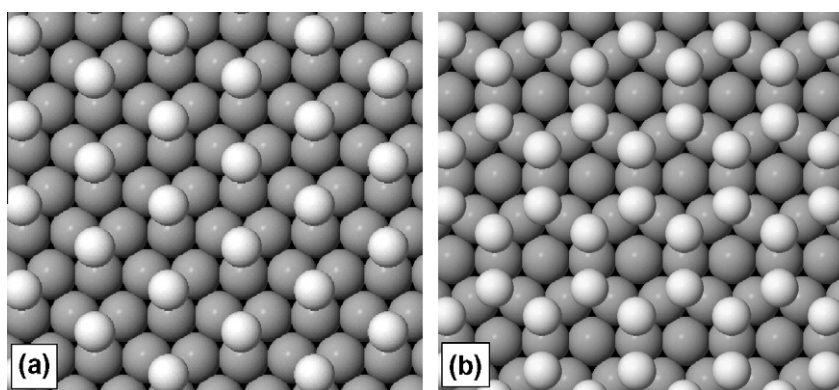


Fig. 1. The  $(\sqrt{3} \times \sqrt{3})R30^\circ$  (a) and the  $(2 \times 2)$  honeycomb (b) structures of Cl on Ag(111).

The present paper is devoted to the study of lateral interaction in Cl layers adsorbed on Ag(111) at low coverages (up to 0.5 ML), when the diffusion of Cl into the bulk is negligible. Specifically, the formation of the Cl structures at different temperatures and order–disorder transitions are simulated by the Monte Carlo method, using the energy parameters of lateral interaction estimated from DFT calculations performed for various distances between adsorbed atoms.

## 2. Methods of calculations

The DFT semirelativistic calculations were carried out with CASTEP code [24], using ultrasoft pseudopotentials [25] and generalized gradient approximation (GGA) with Perdew–Burke–Ernzerhof (PBE) functional for exchange–correlation energy [26]. The surfaces were simulated with the repeated-slab (supercell) model, with Cl atoms adsorbed on one side of the slab. The thickness of the slab was of four layers and the vacuum gap was about 10 Å. The lateral interaction between Cl adatoms on Ag(111) were estimated using a  $(3 \times 3)$  surface unit cell.

Positions of adsorbed chlorine atoms and Ag atoms of two surface layers were optimized (using BFGS [27] optimization procedure) until the forces on atoms converged to less than 0.03 eV/Å. The efficiency of the Brillouin zone sampling, using various  $k$ -point lattices, was verified by increasing the number of  $k$ -points until the required 0.01 eV convergence of the total energy and about 0.01 Å accuracy of atomic positions were achieved ( $3 \times 3 \times 1$  Monkhorst–Pack [28] sets of special  $k$ -points were found sufficient for Ag(111)). All calculations were performed with the cut-off energy of 300 eV.

Before depositing Cl atoms, the slabs were relaxed, that is, all atoms were allowed to adjust their positions to minimize the total energy of the system. The optimization of atomic positions for a clean Ag(111) surface, in agreement with the results of other calculations [19], resulted in the  $\sim 5\%$  contraction of the topmost Ag surface layer with respect to the related interplane distance in a bulk Ag (the estimated lattice constant of the bulk Ag was 4.27 Å in agreement with the previously found value 4.16 Å [19]). Only minor relaxation shifts were found for the second and the third layers. Optimization of atomic positions of adsorbed chlorine atoms along with Ag atoms of the surface layer led, on average, to a backward relaxation shift of the Ag(111) surface.

To evaluate the binding (adsorption) energy, calculations of the total energies were performed for the  $(\sqrt{3} \times \sqrt{3})R30^\circ$  and honeycomb structures on the 4-layer Ag(111) slabs (Fig. 1). The binding energy per Cl atom  $E_b$  (defined to be positive) was found as

$$E_b = -(E_{\text{Ag+Cl}} - E_{\text{Ag}} - nE_{\text{Cl}})/n, \quad (1)$$

where  $E_{\text{Ag+Cl}}$  is the total energy of the system with  $n$  adsorbed Cl atoms in the surface cell,  $E_{\text{Ag}}$  and  $E_{\text{Cl}}$  are total energies of the substrate and Cl atom, respectively.

For the modeling of the formation of chlorine structures on the Ag(111) surface, we used our set of Monte Carlo (MC) programs, verified in simulation for various adsorption systems [23,29,30]. Briefly, the method explores the standard Metropolis algorithm for the lattice gas model with account for long-range interactions between particles adsorbed on the  $60 \times 36$  lattice with periodic boundary conditions. The rearrangement of the particles was performed by movements of randomly chosen adatoms to neighboring sites, taking into account the barrier for surface diffusion.

The probability of a jump,  $\exp(-\Delta E/kT)$ , depends on the difference of energies  $\Delta E$  of lateral interaction with other adsorbed atoms for the initial and final configurations. When the jump leads to a gain in energy ( $\Delta E < 0$ ), or when the estimated probability exceeds a random number, the jump is accomplished. Otherwise the particle remains at the original site. Relative intensities of LEED reflections are estimated within the kinematical approximation:

$$I(h, k) = \left| \sum_n \exp\{2\pi i(hx_n + ky_n)\} \right|^2, \quad (2)$$

where the summation is performed over occupied sites with  $x_n$  and  $y_n$  coordinates, defined in terms of fractions of the simulated fragment of the surface (the part of the surface adopted in the present work contains  $30 \times 36$  atoms of the Ag(111) surface, which roughly corresponds to the coherence width of a typical LEED device). The distribution of LEED reflections was obtained by varying reciprocal space coordinates  $h$  and  $k$ , and estimated relative intensities were depicted by circles with diameters proportional to the intensity of reflections.

## 3. Results

The performed calculations of total energies have shown that, for coverages up to 0.5 ML, triply coordinated (threefold) hollow sites of the Ag(111) surface are strongly favorable for chlorine atoms with regard to other available sites. Specifically, in a good agreement with other DFT calculations [17], the binding energy for Cl adatoms in the threefold sites for the  $(\sqrt{3} \times \sqrt{3})R30^\circ$  structure (Fig. 1a), is found to be of 2.80 eV, which by 0.1 eV exceeds the binding energy of Cl in short-bridge sites. The position of Cl in on-top sites is unstable. The difference between the fcc and hcp hollow sites is found to be less than 0.01 eV, which is within the estimated error bar of calculations. Hence, at low coverages Cl atoms occupy either fcc or hcp threefold sites with the Cl–Ag

bond length of 2.66 Å, which is consistent with previously obtained values of 2.48 Å [5], 2.62 Å [17], and 2.7 Å [14,21].

The relative diameters of the Cl and Ag atoms, appropriate for a ball model, can be estimated from the calculated bond length and the distance between Ag atoms, which is the period of the hexagonal Ag(111) surface, 2.89 Å. Thus, for touching Ag spheres, the radius of Ag atom is defined as 1.45 Å and, as the Cl–Ag bond length is found to be of 2.66 Å, the radius of the Cl adatom in the  $(\sqrt{3} \times \sqrt{3})R30^\circ$  structure is  $\sim 1.2$  Å. The size of the adsorbed Cl noticeably exceeds the 2.0 bondlength in a free Cl<sub>2</sub> molecule, which may be attributed to a certain negative charge acquired by Cl on adsorption. Hence, for a ball model for Cl on Ag(111), it is reasonable to adopt the relative radii of Cl and Ag defined as  $r_{\text{Cl}}/r_{\text{Ag}} = 1.2/1.45 = 0.83$  (approximately this relation was used for the atomic spheres depicted in Fig. 1).

To simulate the formation of Cl structures on the Ag(111) surface by Monte-Carlo method, the energies of lateral interaction should be determined for rather long distances between adatoms (Table 1). The distances between first five nearest neighbor threefold sites (shown in insets in Fig. 2) are of 1.67, 2.89, 3.34, 4.41, 5.01, and 5.78 Å, respectively. It should be noted that the distance between the first nearest neighbor threefold sites is smaller than the distance between the chlorine atoms in a free molecule (2.0 Å), which would lead to a very strong lateral interaction between Cl adatoms being set at such sites. Thus, if the optimization of the atomic positions were performed for the atoms at the distances less than 3.34 Å without any constraints, the chlorine atoms would unavoidably leave the threefold sites, which complicates the estimation of the energy of lateral interaction. For larger Cl–Cl distances, including those characteristic of the  $(\sqrt{3} \times \sqrt{3})R30^\circ$  structure, all adatoms occupy threefold sites without any displacements.

The estimated energies of the lateral interaction between Cl atoms as a function of the interatomic distance are presented in Fig. 2 and Table 1. It might be expected that for sufficiently large distances between adsorbed atoms the lateral interaction could be attributed to the dipole–dipole repulsion. However, the dipole moment of the chlorine atom adsorbed on the silver surface, estimated from the initial slope of the work function dependence on coverage [31], is about 0.75–0.9 Debye, so that for the distances that correspond to the second and the third neighbors the dipole–dipole interaction between adatoms is too weak and therefore cannot explain a rather strong repulsion between Cl adatoms (see Fig. 2). It should be noted in this regard that small work function changes do not necessarily mean small charge transfer [32–34]. In particular, recent DFT calculations by Migani et al. [34] have demonstrated that the change on the surface work function induced by the presence of the adsorbed halide can be either positive or negative, depending on the metal surface. Therefore, one may conclude that the use of the work function change to extract information about the net charge on the adsorbate should be regarded with extreme caution.

**Table 1**

The energies (eV) of the lateral interaction, estimated from DFT-GGA (GGA) calculations for various interatomic distances (Å) between Cl atoms in threefold hollow sites on the Ag(111) surface and parameters used in Monte Carlo simulation (MC) of the formation of the  $(\sqrt{3} \times \sqrt{3})R30^\circ$  structure at  $\theta = 0.33$  and a honeycomb structure at  $\theta = 0.5$ .

Neighbors	Distance	GGA	MC
1st	1.67	5.00	5.00
2nd	2.89	0.72	1.03
3rd	3.34	0.40	0.47
4th	4.41	0.25	0.28
5th	5.01	0.05	0.02
6th	5.78	0	0

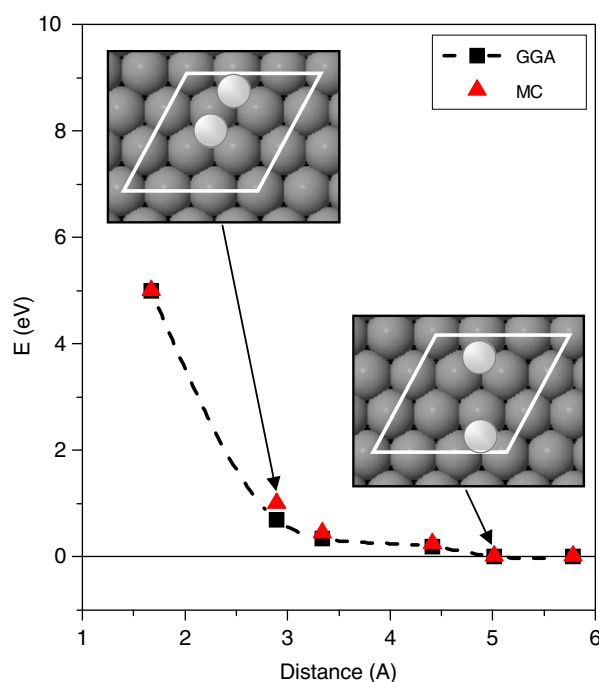


**Fig. 2.** The energies of lateral interaction for various distances between chlorine adatoms in threefold hollow sites on Ag(111). The results of DFT calculations are shown by squares connected by a dash line. Triangles denote parameters used in Monte Carlo simulation.

Hence, the origin of the lateral interaction between adsorbed Cl atoms is of a complex character and, probably, should be attributed to the indirect interaction [35–37], which is accomplished through electrons of the metal substrate and characterized by a non-monotonic (oscillative) dependence on the interatomic distance. With obtained energies of lateral interaction, the formation of the  $(\sqrt{3} \times \sqrt{3})R30^\circ$  structure at  $\theta = 0.33$  was reproduced with the Monte Carlo simulation. However, the temperature of the order–disorder transition was found to be somewhat lower than that found in the experiment [5]. Thus, to obtain a correct order–disorder temperature, the parameters of the lateral interaction for the second and third neighbors (which, as mentioned above, could be found from GGA calculations with a limited accuracy) were slightly modified (see Table 1). The difference between energy values for lateral interactions from DFT-GGA calculations and Monte Carlo fitting to experiment could arise, probably, from the use of the PBE functional in present study. Thus, it seems very likely that calculations within LDA or GGA with the PW91 functional [38] for exchange–correlation might give energies of lateral interactions somewhat closer to the Monte Carlo parameters (the choice of the exchange–correlation potential does play an important role in estimates of work function, structure, and binding energies for Cl on various metal surfaces, as is shown and discussed in detail in Refs. [22,34]).

The modeling of the ordering of the Cl layer at  $\theta = 0.33$  was performed by stepwise decreasing the temperature with the number of diffusion MC steps sufficient to achieve the equilibrium at each temperature. At  $T = 210$  K the layer is disordered and no additional reflections appear in the model LEED pattern (Fig. 3a and b). It is not surprising therefore that for low Cl coverages on Ag(111) no ordered structures have been observed at room temperature [1–5]. At 196 K, the  $(\sqrt{3} \times \sqrt{3})R30^\circ$  structure starts to form, but the presence of domain walls results in a splitting of the reflections thus diminishing their intensities. At  $T = 194$  K the layer abruptly becomes well ordered (Fig. 3c) and provides a sharp LEED pattern

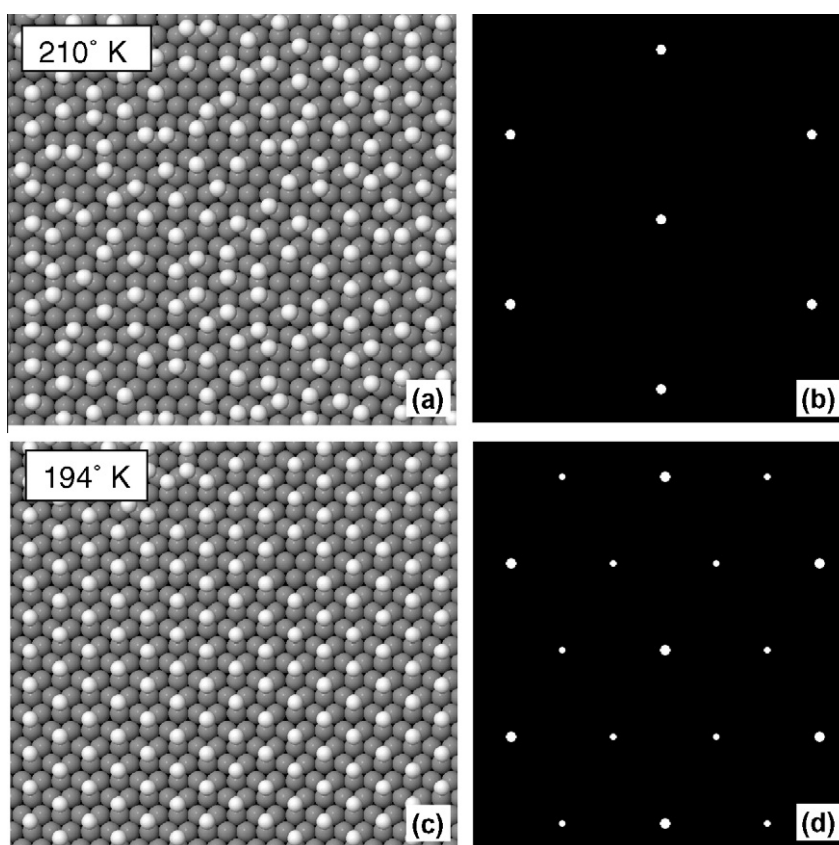


**Fig. 3.** The formation of the  $(\sqrt{3} \times \sqrt{3})R30^\circ$  Cl structure at  $\theta = 0.33$  in Monte Carlo simulation. At  $T = 210$  K the layer is disordered (a) and the LEED pattern (b) has no additional reflections. At  $T = 194$  K the layer abruptly becomes well ordered (c) and provides a sharp  $(\sqrt{3} \times \sqrt{3})R30^\circ$  LEED pattern (d).

(Fig. 3d). A further decrease of the temperature does not lead to any changes in the film structure.

A surface diffusion step may be viewed as a jump of a Cl atom from one to another threefold hollow site over a barrier. The height of the barrier, in principle, could be estimated using the search of the transition point with the NEB method, implemented in CASTEP. In the present case, due to a simple geometry, the transition point for diffusion from one to another threefold adsorption site is just the bridge site between the two, and therefore the method of a step-by-step move of an adsorbed atom from one to a neighboring one, with optimization of the position of the adatom along the normal to the surface [30,39] seems to be more efficient. Thus, the transition point corresponds to the difference between the energies calculated for Cl adatom in the threefold and bridge sites ( $\sim 0.1$  eV, as follows from present DFT calculations).

Because of a restricted mobility, a quality (a degree of order) of obtained structures significantly depends on the actual cooling rate. Thus, when the cooling of the system is relatively slow, the Cl layer condenses, for  $\theta = 0.33$ , into the perfect  $(\sqrt{3} \times \sqrt{3})R30^\circ$  structure (Fig. 4). In particular, the simulated order–disorder transition is very sharp (the temperature range is  $\sim 2$  K), which is in a good agreement with the results of the LEED study of Cl layers adsorbed on Ag(111) [5]. In contrast, when the rate of the decrease of temperature is high, the restricted mobility may lead to formation of separate domains of the  $(\sqrt{3} \times \sqrt{3})R30^\circ$  structure. The LEED pattern, simulated for this structure, demonstrates characteristic reflections with weak satellites, which indicate the splitting of the beams due to the phase shift for electrons scattered from different domains, and, consequently, the intensity of LEED reflections characteristic of the  $(\sqrt{3} \times \sqrt{3})R30^\circ$  structure decreases. For this reason, the sharpness of the disorder-to-order transition depends on the rate of the decrease of temperature (see Fig. 4).

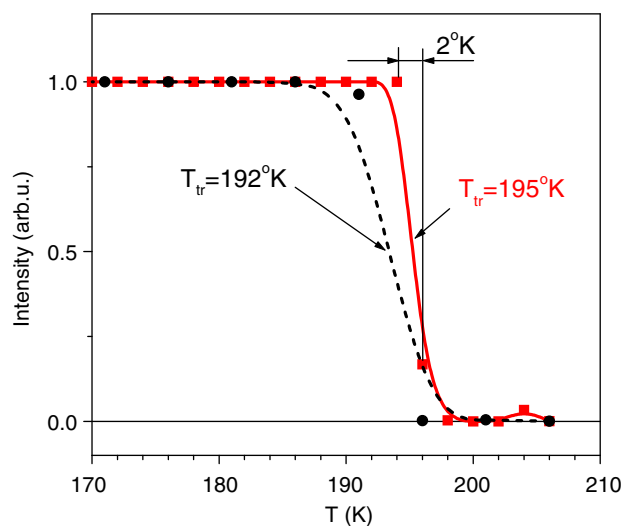


**Fig. 4.** The order–disorder transition diagram for the  $(\sqrt{3} \times \sqrt{3})R30^\circ$  structure at  $\theta = 0.33$ . The sharpness of the transition depends on the rate of cooling, as is illustrated by two plots obtained with Monte Carlo simulation for the 2 K (solid line) and 5 K (dash line) temperature steps.

The diameter of a Cl atom is  $2.4 \text{ \AA}$ , as it was estimated above from the Cl–Ag bondlength in the  $(\sqrt{3} \times \sqrt{3})R30^\circ$  structure, while the lattice period of the Ag(111) surface is of  $2.89 \text{ \AA}$ . Because of a relatively small radius of Cl adatoms they could, in principle, form even a complete  $(1 \times 1)$  monolayer. Therefore, the saturation at the coverage about 0.5 occurs not because of a large diameter of Cl adatom, but originates from a strong lateral repulsion which

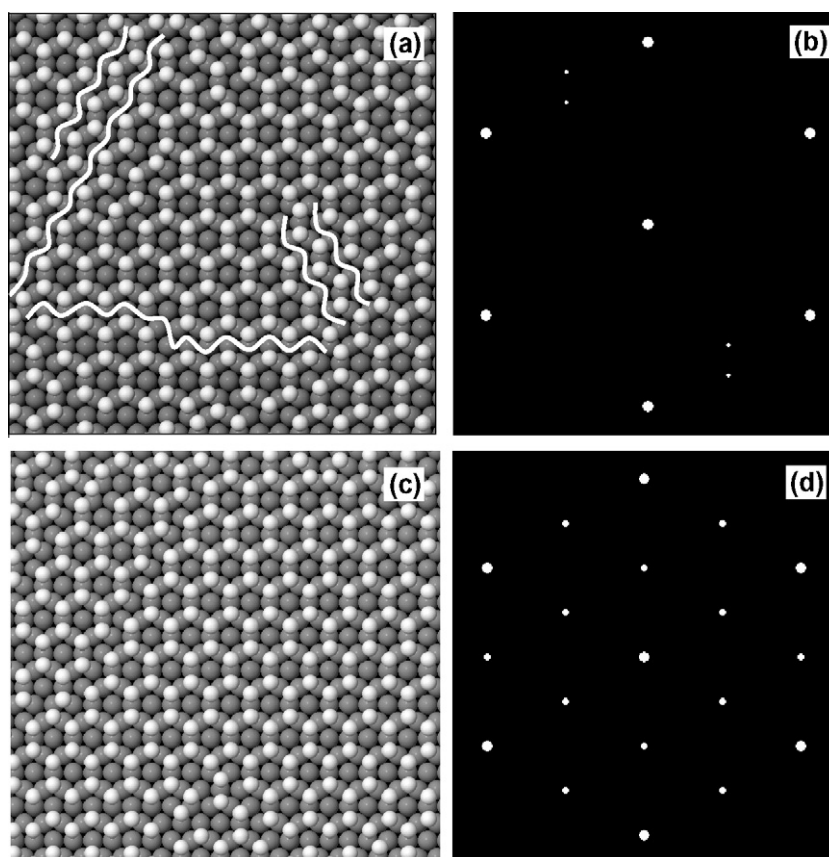


**Fig. 5.** Monte Carlo simulation of Cl structures at  $\theta = 0.5$ . At  $T = 160$  K the honeycomb structure seems to be well ordered (a), but the corresponding LEED pattern (b) does not contain characteristic  $(2 \times 2)$  reflections because of a cancellation due to forming antiphase domains. Some typical domain walls are indicated by zigzag lines. Under special conditions (see text), a large island of the honeycomb structure (c), giving rise to a sharp  $(2 \times 2)$  LEED pattern (d), can be formed.

significantly lowers an effective energy of adsorption. This view might seem unusual comparing with a commonly accepted picture where large Cl atoms are deposited on small Ag atoms composing the surface, but can be further argued by consideration of two characteristic features of Cl on Ag(111): (i) For increased temperatures and high expositions Cl atoms diffuse into the substrate, which would be impossible if the Cl atoms were larger than Ag; (ii) the sharpness of the order–disorder transition for the  $(\sqrt{3} \times \sqrt{3})R30^\circ$  structure ultimately indicates that there should be a sufficient space for the two-dimensional evaporation of the Cl adatoms (recall that in the case of dense structures forming nearly at saturation coverages the transition is rather smooth on the temperature scale). Indeed, along the disordering, Cl adatoms should unavoidably occur at the distance that correspond to the lattice period of the Ag(111) surface, 2.89 Å.

The DFT calculations [19,21] predict that at  $\theta = 0.5$  chlorine on Ag(111) should form a hexagonal honeycomb structure (Fig. 1b), which is the most favorable due to maximal interatomic distances between the Cl adatoms. Nonetheless, the formation of the honeycomb structure has not been observed in LEED studies yet. The absence of the related  $(2 \times 2)$  pattern is usually attributed to a large radius of Cl, and it is believed therefore that close to the saturation coverage,  $\theta \sim 0.5$ , only coincidence (incommensurate) hexagonal structures like  $(10 \times 10)$  [2],  $(13 \times 13)$  [5], or  $(17 \times 17)$  [4] may be formed on the Ag(111) surface. However, the repulsion between Cl adatoms for the distance specific for the  $(2 \times 2)$  honeycomb structure (which corresponds to the third nearest neighbors in Fig. 2) is not strong enough to preclude its formation. Hence, there are no obvious objections for the formation of the honeycomb

structure, and the absence of the corresponding  $(2 \times 2)$  LEED pattern needs an explanation.

The Monte Carlo modeling of the ordering of the Cl layer at  $\theta = 0.5$  was performed by decreasing the temperature (similarly to the simulation of the formation of the  $(\sqrt{3} \times \sqrt{3})R30^\circ$  structure). At room temperature the layer is found to be disordered, but with decreasing temperature down to 200 K some fragments of the honeycomb structure start to form, and at  $T \approx 160$  K the layer becomes seemingly ordered (Fig. 5a), and with the further decrease of temperature the structure of the Cl layer does not change. It could be expected that the LEED pattern corresponding to the ordered layer would show the  $(2 \times 2)$  lattice; in fact, however, only some weak splitted reflections appear in the calculated pattern (Fig. 5b). This is a result of phase shifts for the electron scattering on the domains, which leads to the cancellation of the characteristic LEED reflections. Hence, we predict that the  $(2 \times 2)$  LEED pattern cannot be seen in experiment, because at room temperature the structure is disordered, while at low temperatures the  $(2 \times 2)$  pattern is absent because of forming antiphase domains and a low mobility of domain boundaries (domain walls, or solitons, shown in Fig. 5a).

However, at special conditions, large islands having the  $(2 \times 2)$  honeycomb structure can be grown. In simulations, this can be accomplished with the same set of the parameters of the lateral interaction as above, but with a very slow decrease of temperature, starting from different initial states (temperatures and random structures). The example of a well ordered honeycomb structure, presented in Fig. 5c, which provides the  $(2 \times 2)$  LEED pattern (Fig. 5d), illustrates the possibility of the formation of large domains of the  $(2 \times 2)$  honeycomb structure in principle, which, in

fact, seems to be rather improbable in real experiments. Thus, the absence of the  $(2 \times 2)$  LEED pattern for Cl on Ag(111) at  $\theta = 0.5$  does not indicate the lack of the forming islands with the honeycomb structure, which nevertheless could be seen in STM images obtained at low ( $\sim 160$  K) temperatures.

#### 4. Conclusion

We have studied lateral interactions in Cl layers adsorbed on Ag(111) at low coverages (up to 0.5 ML), when the diffusion of Cl into the bulk is negligible. The energy parameters of the lateral interaction have been estimated from DFT calculations performed for various distances between adsorbed atoms. It has been found that the formation of the  $(\sqrt{3} \times \sqrt{3})R30^\circ$  and honeycomb Cl structures can be reproduced in the Monte Carlo simulation with parameters of lateral interaction estimated from DFT calculations. In particular, it has been shown that the transition is very sharp due to a sufficient number of free adsorption sites and substantial repulsive lateral interaction between adatoms.

The height of the diffusion barrier of 0.1 eV, estimated from the difference between the chemisorption energies in the hollow and bridge sites, indicates a restricted mobility of adatoms, which is found to be essential for formation of the ordered film structures. In particular, a quality (a degree of order) of obtained structures significantly depends on the actual cooling rate. For imperfect domain structures the model LEED patterns show a characteristic splitting or even cancellation of the reflections due to the phase shift for electrons scattered at different domains. It is very likely that the forming domains of the  $(2 \times 2)$  honeycomb structure for Cl coverages on Ag(111) about 0.5 can be observed by a low-temperature STM, while the absence of the  $(2 \times 2)$  LEED pattern should be attributed to the formation of antiphase domains of the structure, which results in the cancellation of characteristic LEED reflections.

#### Acknowledgements

We wish to express our gratitude to B. Andryushechkin and K. Eltsov for helpful discussions. This work was supported in part by the Ukrainian-Russian NASU/RFBF Grant No. RFFD/3-10-26.

#### References

- [1] G. Rovida, F. Pratesi, *Surf. Sci.* 51 (1975) 270.
- [2] P.J. Goddard, R.M. Lambert, *Surf. Sci.* 67 (1977) 180.
- [3] M. Bowker, K.C. Waugh, *Surf. Sci.* 134 (1983) 639.
- [4] B.V. Andryushechkin, K.N. Eltsov, V.M. Shevlyuga, V.Yu. Yurov, *Surf. Sci.* 407 (1998) L633.
- [5] A.G. Shard, V.R. Dhanak, *J. Phys. Chem. B* 104 (2000) 2743.
- [6] C.T. Campbell, M.T. Paffett, *Appl. Surf. Sci.* 19 (1984) 28.
- [7] R.A. Marbrow, R.M. Lambert, *Surf. Sci.* 71 (1978) 107.
- [8] Y.Y. Tu, J.M. Blakely, *Surf. Sci.* 85 (1979) 276.
- [9] M. Kitson, R.M. Lambert, *Surf. Sci.* 100 (1980) 368.
- [10] M. Bowker, K.C. Waugh, B. Wolfendale, G. Lambie, D.A. King, *Surf. Sci.* 179 (1987) 266.
- [11] B.V. Andryushechkin, K.N. Eltsov, V.M. Shevlyuga, *Surf. Sci.* 109 (1999) 433.
- [12] B.V. Andryushechkin, K.N. Eltsov, V.M. Shevlyuga, V.Yu. Yurov, *Surf. Sci.* 96 (1999) 431.
- [13] B.V. Andryushechkin, V.V. Cherkez, E.V. Gladchenko, G.M. Zhidomirov, B. Kirren, Y. Fagot-Reverat, D. Malterre, K.N. Eltsov, *Phys. Rev. B* 81 (2010) 205434.
- [14] G.M. Lambie, R.S. Brooks, S. Ferrer, D.A. King, D. Norman, *Phys. Rev. B* 34 (1986) 2975.
- [15] J.H. Schott, H.S. White, *J. Phys. Chem.* 98 (1994) 291.
- [16] H. Piao, K. Adib, M.A. Barteau, *Surf. Sci.* 557 (2004) 13.
- [17] K. Doll, N.M. Harrison, *Phys. Rev. B* 63 (2001) 165410.
- [18] Y. Wang, Q. Sun, K. Fan, J. Deng, *Chem. Phys. Lett.* 334 (2001) 411.
- [19] N.H. de Leeuw, C.J. Nelson, C.R.A. Catlow, P. Sautet, W. Dong, *Phys. Rev. B* 69 (2004) 045419.
- [20] A. Migani, F. Illas, *J. Phys. Chem. B* 110 (2006) 11894.
- [21] P. Gava, A. Kokalj, S. Gironcoli, S. Baroni, *Phys. Rev. B* 78 (2008) 165419.
- [22] A. Roldán, D. Torres, J.M. Ricart, F. Illas, *Surf. Sci.* 602 (2008) 2639.
- [23] N.V. Petrova, I.N. Yakovkin, *Phys. Rev. B* 76 (2007) 205401.
- [24] S.J. Clark, M.D. Segall, C.J. Pickard, P.J. Hasnip, M.J. Probert, K. Refson, M.C. Payne, *Z. Kristallogr.* 220 (2005) 567.
- [25] D. Vanderbilt, *Phys. Rev. B* 41 (1990) 7892.
- [26] J.P. Perdew, K. Burke, M. Ernzerhof, *Phys. Rev. Lett.* 77 (1996) 3865.
- [27] B.G. Pfrommer, M. Cote, S.G. Louie, M.L. Cohen, *J. Comput. Phys.* 131 (1997) 133.
- [28] H.J. Monkhorst, J.D. Pack, *Phys. Rev. B* 13 (1976) 5188.
- [29] N.V. Petrova, I.N. Yakovkin, Yu.G. Ptushinskii, *Eur. Phys. J. B* 38 (2004) 525.
- [30] N.V. Petrova, I.N. Yakovkin, *Surf. Sci.* 578 (1–3) (2005) 162.
- [31] K. Wu, D. Wang, J. Deng, X. Wei, Y. Cao, M. Zei, R. Zhai, Z. Gao, *Surf. Sci.* 264 (1992) 249.
- [32] L.G.M. Pettersson, P.S. Bagus, *Phys. Rev. Lett.* 56 (1986) 500.
- [33] A. Michaelides, P. Hu, M.-H. Lee, A. Alavi, D.A. King, *Phys. Rev. Lett.* 90 (2003) 246103.
- [34] A. Migani, C. Sousa, F. Illas, *Surf. Sci.* 574 (2005) 297.
- [35] T.B. Grimley, *Proc. Phys. Soc. (Lond.)* 92 (1967) 776.
- [36] T.L. Einstein, *CRC Crit. Rev. Sol. St. and Mat. Sci.* 7 (1978) 261; K.H. Lau, W. Kohn, *Surf. Sci.* 75 (1978) 69.
- [37] O.M. Braun, V.K. Medvedev, *Sov. Phys. Usp.* 32 (1989) 328.
- [38] J.P. Perdew, J.A. Chevary, S.H. Vosko, K.A. Jackson, M.R. Pederson, D.J. Singh, C. Fiolhais, *Phys. Rev. B* 46 (1992) 6671.
- [39] I.N. Yakovkin, N.V. Petrova, *Appl. Surf. Sci.* 254 (2008) 4258.